ACS Macro Letters

Letter

pubs.acs.org/macroletters

Percolation, Tie-Molecules, and the Microstructural Determinants of Charge Transport in Semicrystalline Conjugated Polymers

Sonya A. Mollinger,[†] Brad A. Krajina,[‡] Rodrigo Noriega,[§] Alberto Salleo,[∥] and Andrew J. Spakowitz*[,†,‡,∥,⊥]

[†]Department of Applied Physics, [‡]Department of Chemical Engineering, [∥]Department of Materials Science and Engineering, and [⊥]Biophysics Program, Stanford University, 450 Serra Mall, Stanford, California 94305, United States

[§]Department of Chemistry, University of California at Berkeley, Berkeley, California, United States

Supporting Information

ABSTRACT: Semiconducting polymers play an important role in a wide range of optical and electronic material applications. It is widely accepted that the polymer ordering impacts charge transport in such devices. However, the connection between molecular ordering and device performance is difficult to predict due to the current need for a mathematical theory of the physics that dictate charge transport in semiconducting polymers. We present an analytical and computational description of semicrystalline conjugated polymer materials that captures the impact of polymer conformation on charge transport in heterogeneous thin films. We first develop an analytical theory for the statistical behavior of a polymer chain emanating from a crystallite, predicting the average distance to the first kink that would trap a charge. This analysis is used to define the conditions where percolation would lead to efficient transport through a semicrystalline material. We then establish a model that predicts the multiscale charge transport. This model is used to identify the speed limits of charge transport at short and long time scales for varying fraction of crystallinity. This work provides a rational framework to connect molecular organization to device performance.

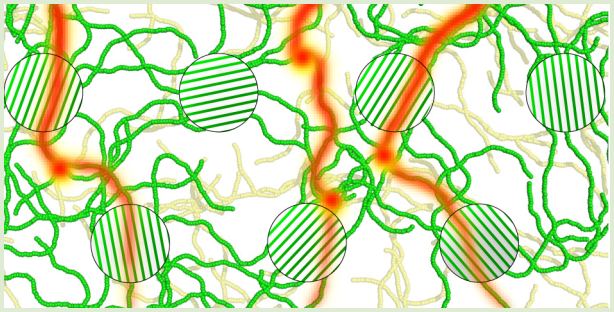

Semiconducting polymers are currently under extensive investigation for applications in solar cells,[1] light-emitting diodes,[2] flexible electronics,[3] and biointerfacing.[4] The use of polymers offers a number of advantages over traditional silicon devices, including flexibility, inexpensive processing, and the ability to functionalize the materials for various chemical interactions. Performance has substantially improved in recent years due to new materials development and improved processing techniques.[5,6] Films that result in the highest performance typically have a complex semicrystalline morphology,[7] indicating that considerable performance improvement can be achieved through optimization of microstructural properties. To rationally design new materials, it is critical to establish a predictive model that relates the microstructure of a polymer film to its transport properties.

Semiconducting polymer thin films usually have ordered phases with varying degrees of crystallinity scattered throughout an amorphous polymer matrix. Crystalline areas of the film are often composed of molecules cofacially stacked in one direction to give overlap of π-orbitals as well as side chains that organize in a perpendicular direction.[8] It is experimentally suggested that efficient transport in such films occurs via connected networks of crystallites.[9]

In a previous work, we describe transport in the disordered regions of the polymer starting from a model of chain conformations.[10] Our model distinguishes between on-chain and interchain transport, in contrast to widely used Gaussian disorder models, which describe transport as hopping through a spatially and energetically disordered grid of sites.[11−13] Common features of transport in amorphous polymers such as the Poole-Frenkel electric-field dependence[14] and the observed time-dependent mobility[15] are well described using our polymer-based model.[10] Our theoretical description is based on physically motivated and experimentally measurable polymer parameters, enabling a predictive approach to modeling charge transport of such materials.

In this work, we develop a description of semicrystalline polymer films that is based on the interplay between the physical properties of the disordered regions and the scattered crystallites. We show that this model can explain the percolation behavior of charge mobility as the crystallinity of the film increases due to connected networks of crystallites. We analyze the behavior of the tie-molecules between crystallites to identify conditions for percolation in the film and define speed limits for charge transport based on specific microstructural properties.

We develop a model for charge transport in semicrystalline conjugated polymer thin films, shown schematically in Figure 1.

Received: May 12, 2015
Accepted: June 17, 2015
Published: June 22, 2015

DOI: 10.1021/acsmacrolett.5b00314
ACS Macro Lett. 2015, 4, 708−712

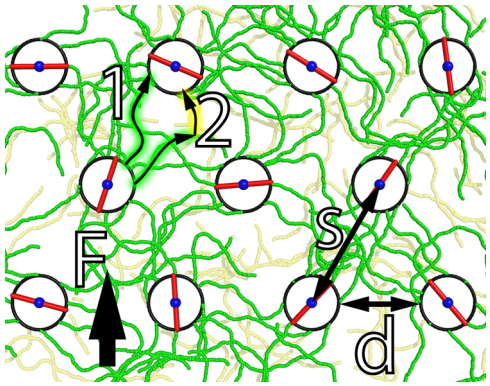

Figure 1. Schematic representation of our model showing an array of crystallites (black circles with center-to-center separation s and intercrystallite spacing d) whose orientations are indicated by the red lines. The green chains indicate polymers within the amorphous region that emanate from a crystal, and the yellow chains are amorphous polymers that do not emanate from a crystallite. The external field F drives charge through the semicrystalline material. Path 1 indicates a direct tie line between two crystallites, and path 2 shows a charge-transport trajectory with a kink, requiring interchain hopping.

The thin film is approximated as a two-dimensional (2D) material with crystallites that are arranged on a triangular lattice with center-to-center spacing s. The intercrystallite spacing d results in a fraction crystallinity $f = (\pi/(2\sqrt{3}))(1 - d/s)^2$. Our simple model for the crystallite size, shape, and arrangement can be replaced by a detailed description that incorporates microstructural heterogeneity that is experimentally determined or theoretically predicted. However, our simple approach enables us to analyze the dominant effects of microstructure and percolation on charge transport. The orientation of each crystallite is assumed to be random, indicated by the red lines in Figure 1. Thus, the orientations of adjacent crystallites are not correlated.

We describe the amorphous regions of a semicrystalline film with a 2D analogue of our model of amorphous charge transport.[10] The chain conformations are generated using the wormlike chain (WLC) model,[16,17] where the polymer resists bending deformation between each monomer and is subjected to thermal fluctuations with energy k_BT. The persistence length l_p scales with the bending rigidity and dictates the length of chain over which the chain orientation remains correlated. We use a discrete representation of the WLC with discretization length l_0, resulting in the bending energy

$$E_{\text{bend}} = k_BT\epsilon \sum_{i=1}^{N-1} (1 - \vec{u}_{i+1}\cdot\vec{u}_i) \tag{1}$$

where $\vec{u}_i$ is the tangent orientation of the ith segment, N are the number of segments in the chain, and $\epsilon = l_p/l_0$ is the bending rigidity. A chain that emanates from a crystallite (e.g., green chains in Figure 1) has an initial orientation that is given by the orientation of the crystallite. A chain that does not emanate from a crystallite (e.g., yellow chains in Figure 1) has a random initial orientation. Each chain conformation is selected from a Boltzmann distribution and subsequently frozen in space, assuming the conformations in the amorphous region are vitrified.

Before incorporating charge transport into the model, it is instructive to explore the connectivity between crystallites. There are two types of paths along which the charges travel between crystalline regions. In the first path type, a charge travels directly on a connecting chain, referred to in this work as a tie-molecule, from one crystallite to another (illustrated as path 1 in Figure 1). In the second path type, a charge travels along a chain in the amorphous phase until it reaches a kink in the chain, at which point it must pause until it is able to hop to a different chain and continue to the next crystalline region (illustrated as path 2 in Figure 1). The transport along path 2 is significantly slower than that along path 1. Thus, it is important to identify the conditions that allow for a significant number of tie-molecules and thereby enable the faster transport of path 1.

A tie-molecule occurs when intercrystallite spacing d does not include a kink in the chain with respect to the field direction. We develop an analytical theory to calculate the average distance a chain extends before a kink occurs. We define a kink to be the chain position where the tangent vector becomes perpendicular to the field direction. The total displacement will additionally depend on the initial orientation of the chain θ_0. The conformational statistics are determined by a constrained Green's function

$$G_c(\theta|\theta_0;\, L) = \frac{2}{\pi} \sum_{m=1}^{\infty} \sin(m\theta)\sin(m\theta_0)e^{-m^2L/(2l_p)} \tag{2}$$

that gives the probability that a chain segment of length L with an initial orientation θ_0 has a final orientation θ with no kinks along the segment length L. The average displacement before reaching a trap is obtained using the constrained Green's function G_c. The average displacement for a chain with a kink at segment length L is determined for an initial orientation θ_0 (dictated by the crystallite orientation) and a final orientation θ that is perpendicular to the field. This average displacement is statistically weighted by the probability of having the kink at segment length L, and the total average displacement is determined by integrating over all chain lengths. The details are shown in the Supporting Information. More generally we note that this technique of constraining the statistics of polymer chains and analyzing the resulting set of conformations can be widely applied to problems involving constrained geometries.

Figure 2 visualizes this result. A semicrystalline film is shown for different combinations of bending modulus ϵ and fraction crystallinity f. The red curves indicate the calculated displacement along the chain before reaching a trap. As the bending modulus of the chains increases, the average length of the chains in the field direction also increases, leading to an elongation of the red curves. Additionally, as we increase the fraction of crystallites in the film, the distance to a trap correspondingly increases relative to the intercrystallite spacing d, and the probability of a chain connecting two crystallites also increases. For smaller fraction crystallinity, the persistence length must be significantly larger to obtain continuous transport by avoiding traps between crystallites. Similarly, even at high crystallite fractions, chains with a persistence length slightly higher than the monomer length are barely able to connect crystals. The controlling parameter for continuous transport is therefore the ratio of persistence length to intercrystallite spacing l_p/d.

We quantitatively model the transport in a film with both amorphous and crystalline regions using dynamic Monte Carlo simulations. We incorporate the circular crystallites of Figure 1 with a transport model based on the 2D WLC. Each crystallite is randomly oriented with a direction of high mobility and a perpendicular direction of lower mobility, corresponding to the

DOI: 10.1021/acsmacrolett.5b00314
ACS Macro Lett. 2015, 4, 708−712

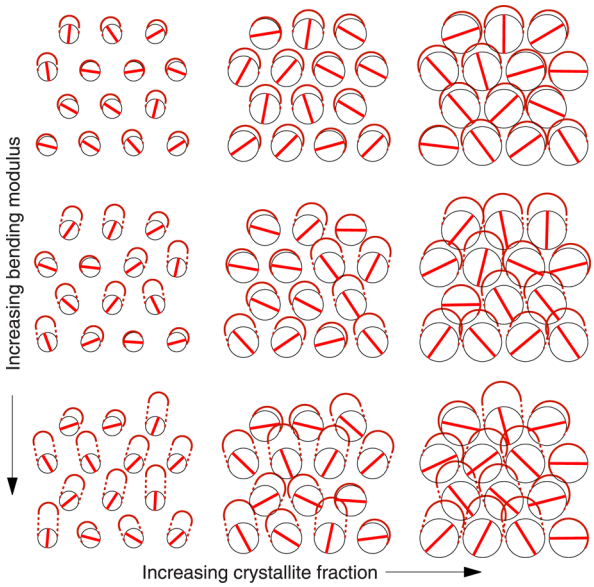

Figure 2. Visualization of the distance charges travel after exiting a crystallite before reaching a morphological trap, for three different values of bending modulus and fraction crystallinity. The red lines indicate the orientations of the crystallites, and the field is in the vertical direction. The red curves represent the average distance that the chain extends before a trap occurs. Overlap of the red-outlined cones with crystallites indicate the existence of tie-molecules.

backbone and π-stacking directions, respectively. Inter- and intrachain hopping rates are determined using a field-dependent Marcus theory between adjacent sites on a polymer chain.[18] We use approximately the set of on-chain and interchain parameters as were fit to experimental data in ref 10 (J_0 = 0.08 eV, λ_0 = 0.6 eV, γ = 5, J_{hop} = 0.00035 eV, λ_{hop} = 0.8 eV, and l_0 = 1 nm). Charge movement in the crystallites is characterized by two fixed mobility values $\mu_{\parallel}$ = 0.03 cm^2/(V s) and $\mu_{\perp}$ = 0.003 cm^2/(V s) rather than hopping transport,[19] where the low values used here account for imperfections in the crystallites. Our 2D model aims to capture the behavior in a typical transistor geometry in which mobilities are experimentally measured. However, our previous modeling efforts of charge transport in amorphous materials utilize a three-dimensional (3D) version of the model.[10] The 3D and 2D models exhibit qualitatively similar behaviors for purely amorphous transport. In the case of polycrystalline materials, the quantitative nature of the connections between crystallites will change due to the differences between intercrystallite separation and geometry for 2D and 3D materials.

Mobility from short to long time scales is calculated by tracking the dynamics of charges moving through an ensemble of films (i.e., averaged over film realizations). A simulation of a charge moving through a single film realization involves the following procedure. For a charge starting in an amorphous region, the initial chain conformation is generated, and the charge chooses hopping sites and times with probabilities as determined by the hopping rates. The charge continues to move until it either jumps to an adjacent chain in the amorphous region or it encounters a crystallite. If a charge jumps to an adjacent chain, the new conformation is generated, and the process is repeated until the charge reaches a crystallite. We assume that the charge has entered a crystallite when it crosses the boundary of a grid point (the black circles of Figure 1). In the crystalline phase, the movement of the charge is calculated deterministically through a mobility tensor that combines the external field direction with the crystal orientation using the parallel and perpendicular mobilities. Upon leaving the crystallite, a WLC that begins in alignment with the crystal orientation is generated. The motion is repeated for a specified length of time. We treat charge motion along grain boundaries with the same framework: a charge at the edge can either continue along the exit chain or hop back into the crystal.

In Figure 3 we show the time-dependent mobility for semicrystalline films with crystal fractions varying from f = 0.0−

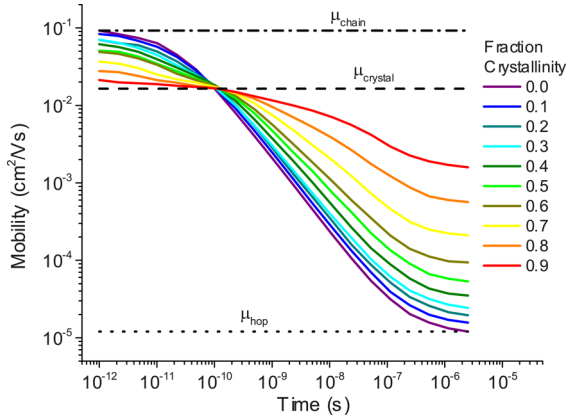

Figure 3. Mobility for different areal coverage of crystallites from picoseconds to microseconds. The dashed line indicates the crystal mobility, the dashed-dotted line is the on-chain mobility, and the dotted line is the interchain hopping mobility.

0.9 (the 2D circle packing limit is f = 0.907) for F = 0.075 V/nm and temperature 300 K. Three relevant mobility values are evident. In the purely amorphous case (f = 0.0), at very short times the transport occurs with an on-chain mobility μ_{chain}, denoted by the dashed-dotted line. At longer times on the order of 1 μs, a second mobility μ_{hop} is reached that includes the effect of the much slower interchain hopping process in amorphous polymer films.[10] This "inter-chain" mobility μ_{hop} is marked by the dotted line, which is nearly 4 orders of magnitude lower than the on-chain mobility μ_{chain} for the chosen parameters. Finally, the dashed line marks the value of the crystalline mobility $\mu_{crystal} = (\mu_{\parallel} + \mu_{\perp})/2$, which is the mobility averaged over crystal orientations with respect to the applied field. At both short and long times, the films that are highly crystalline are predominantly influenced by the crystalline mobility $\mu_{crystal}$. On-chain mobilities are measured at very short times to reach values of 0.01−1 cm^2/V s,[20−22] while mobilities in crystallites are expected to account for crystallite disorder.[7] Varying the relative values of crystal mobility, on-chain mobility, and interchain hopping will result in different time-dependent trends. In particular, as the crystal mobility approaches the on-chain mobility, the short-time values for all films reach the on-chain mobility (see Figure S1 in the Supporting Information).

As we increase the percent crystallinity in the film, the long-time mobility (at 1.0 μs) is plotted for three different values of bending modulus in Figure 4 for fixed applied field. We see an onset of percolation at a percentage of crystallinity that varies with bending modulus. Below some critical percolation value, the long-time mobility remains low. Above this value, the mobility increases up to 2 orders of magnitude for the chosen

DOI: 10.1021/acsmacrolett.5b00314
ACS Macro Lett. 2015, 4, 708−712

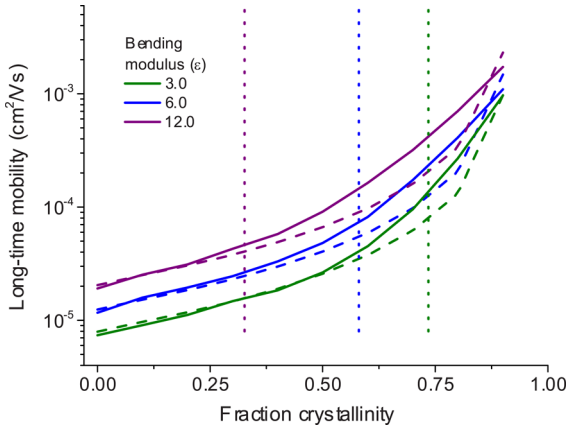

Figure 4. Long-time mobility for different values of bending modulus ϵ. The dotted lines indicate the fraction crystallinity values that give an intercrystallite distance equal to the persistence length of the polymer. The dashed lines represent the conceptual conductivity model described in the text.

parameters. The crystal orientations here are uncorrelated. Introducing correlations should increase the effects shown in Figure 4 by reducing traps at misoriented grain boundaries. Additionally, for sufficiently large fraction crystallinity, including correlations will likely produce anisotropic mobility results, depending on the orientation of the field with respect to the crystallites. This corresponds to experimental results on mobility measured parallel and perpendicular to experimental alignment directions. Future work will explore the influence of alignment and orientation correlation between crystallites on the charge transport.

Transport in semicrystalline polymers[7,23] has been shown experimentally to depend in a complex manner on morphology. It is increasingly possible to control the morphology of polymer films through processing methods, for example, by solution-shearing,[24] mechanical rubbing,[25] or epitaxial growth on organic crystal substrates.[26]

By varying the percent crystallinity in the film over time, Duong et al.[9] have demonstrated that the mobility will show a sharp increase at an onset crystallinity value, consistent with our model. This onset value was measured to correspond to the point when the distance between the crystallites d is approximately equal to the persistence length l_p. In Figure 4, the vertical lines represent the percent crystallinity at which the intercrystallite spacing equals the persistent length of our simulated chains ($d = l_p$). These lines correspond approximately to the value at which the mobility begins to significantly increase or the onset of percolation.

Our model theoretically captures the complex behavior of semicrystalline films shown by experiment. The concept of tie-molecules connecting crystalline regions has been explored experimentally. Here, we show that by modeling the connecting amorphous regions as wormlike chains and using a simple grid of crystalline regions, we can recreate the basic behavior of crystallite percolation via single connecting polymer chains. This theory opens up avenues to explore the complex effects of molecular weight, polydispersity, and applied electric field on charge mobility. In the case of molecular weight, initial results of our theory show a characteristic increase of mobility with molecular weight and then a plateau that is reflected in experimental data.[7] The relationship of this plateau to the persistence length of the polymer is furthermore a function of the details of the crystallite morphology and the electric field. Furthermore, instances of chain ends breaking the tie-molecules dramatically influences the predicted mobility. These effects will be explored in more detail in future work.

In accordance with traditional models of percolation and conductivity,[27,28] we can describe the overall conductivity of the film by adding resistances of the different phases in series or in parallel. There are three contributions to the overall resistance in the film and therefore to the shape of Figure 4. The first is the resistance of the crystallites, which contributes an overall $f/\mu_{crystal}$ in series. We write the contribution of each polymer similarly as proportional to $1/\mu_{chain}$. Finally, the resistance of hopping between chains can be thought of as the resistance of the medium, so we have an additional contribution $\sim 1/\mu_{hop}$, where $\mu_{hop} \ll \mu_{crystal} \ll \mu_{chain}$. Each of these resistances must be multiplied by different scaling factors indicating the proportion of current that flows through each one.

For reasonably high fields, we make an analogy to traditional bond percolation models. We consider two crystallites connected by a single chain as forming a bond with conductivity μ_{chain} with some probability p_c that depends on the fraction crystallinity. Alternatively, the crystallites must be connected by an interchain hop and therefore the bond has a conductivity μ_{hop} with probability $1 - p_c$. We can approximately calculate the probability of forming a bond for some minimum intercrystallite spacing d as equal to the probability that there is a trapless chain of at least length d,

$$p_c = P(d) = \left(\frac{2}{\pi}\right)^2 \int_0^{\pi} \int_0^{\pi} G_c(\theta|\theta_0;\, d)\mathrm{d}\theta\mathrm{d}\theta_0 \tag{3}$$

Then, we can write the mobility (here proportional to conductivity) as

$$\mu = \frac{1}{f/\mu_{crystal} + (1-f)[p_c/\mu_{chain} + (1-p_c)/\mu_{hop}]} \tag{4}$$

where the factor of f is the fraction of crystalline polymer area. The resulting predicted values of mobility are shown as the dotted lines in Figure 4. There is strong agreement in the shape of the corrresponding curves, indicating the above argument is reasonable. At larger field strengths, the model coincides with the simulations at all values of crystallinity (not shown), indicating that our calculation of the connection probability p_c describes charge motion almost perfectly in the limit of high field. At the slightly lower fields at which devices are operated, charges are able to navigate around the occasional kink and percolate at lower fraction crystallinity.

Previous theoretical discussions of conductivity in conducting or semiconducting polymers have taken several forms. The transport in energetically disordered polymer films can be described as a network of varying resistances where the specific resistance of each bond relates to the energetic distance from the Fermi level.[29,30] This description offers an understanding of critical conductance parameters but less insight on the physical microstructure. Carbone et al.[31] describe inter- and intrachain limits for a coarse-grained diffusion model in the absence of a field, while Hu et al.[32] describe conduction through Gaussian coil polymer solutions assuming that junctions between different chains are rapidly connected. Our approach builds on these works by providing a direct connection between the microstructure and the transport behavior driven by an external field.

DOI: 10.1021/acsmacrolett.5b00314
ACS Macro Lett. 2015, 4, 708−712

In conclusion, we have shown that percolation of charge transport between crystallites in a semicrystalline semiconducting polymer is based directly on the properties of tie-molecules. We use dynamic Monte Carlo simulations to model the multiscale charge mobility for films of varying crystallite fractions. We observe three time scales relevant to charge transport in these materials: transport through the crystal, transport along the chain, and transport due to slow interchain hopping. At long time scales and low fraction crystallinity, the last mobility dominates, while at long times and higher fraction crystallinity, the on-chain mobility limits transport. Studying chain conformations analytically allows us to determine the displacement of charges before reaching a kink in the chain, resolving the statistical probability of forming tie-molecules that mark the onset of percolation that dramatically enhances device performance.

■ ASSOCIATED CONTENT

Supporting Information

A discussion of the parameters used and a derivation of the equations used in Figure 2. The Supporting Information is available free of charge on the ACS Publications website at DOI: 10.1021/acsmacrolett.5b00314.

■ AUTHOR INFORMATION

Corresponding Author

*E-mail: ajspakow@stanford.edu.

Notes

The authors declare no competing financial interest.

■ ACKNOWLEDGMENTS

A.J.S. and B.A.K. gratefully acknowledge financial support from Department of Energy, Office of Basic Energy Sciences, Division of Materials Sciences and Engineering, under Contract DE-AC02-76SF00515. S.M. is supported by a Benchmark Stanford Graduate Fellowship. A.S. acknowledges financial support from NSF Award DMR 1205752.

■ REFERENCES

(1) Hoppe, H.; Sariciftci, N. S. *J. Mater. Res.* **2004**, *19*, 1924−1945.
(2) Vohra, V.; Giovanella, U.; Tubino, R.; Murata, H.; Botta, C. *ACS Nano* **2011**, *5*, 5572−5578.
(3) Sekitani, T.; Zschieschang, U.; Klauk, H.; Someya, T. *Nat. Mater.* **2010**, *9*, 1015−1022.
(4) Schwartz, G.; Tee, B. C.-K.; Mei, J.; Appleton, A. L.; Kim, D. H.; Wang, H.; Bao, Z. *Nat. Commun.* **2013**, *4*, 1859.
(5) Lei, T.; Dou, J.-H.; Pei, J. *Adv. Mater.* **2012**, *24*, 6457−6461.
(6) Terao, J.; Wadahama, A.; Matono, A.; Tada, T.; Watanabe, S.; Seki, S.; Fujihara, T.; Tsuji, Y. *Nat. Commun.* **2013**, *4*, 1691.
(7) Noriega, R.; Rivnay, J.; Vandewal, K.; Koch, F. P. V.; Stingelin, N.; Smith, P.; Toney, M. F.; Salleo, A. *Nat. Mater.* **2013**, *12*, 1038−1044.
(8) Rivnay, J.; Mannsfeld, S. C. B.; Miller, C. E.; Salleo, A.; Toney, M. F. *Chem. Rev.* **2012**, *112*, 5488−5519.
(9) Duong, D. T.; Ho, V.; Shang, Z.; Mollinger, S.; Mannsfeld, S. C.; Dacuña, J.; Toney, M. F.; Segalman, R.; Salleo, A. *Adv. Funct. Mater.* **2014**, *24*, 4515−4521.
(10) Noriega, R.; Salleo, A.; Spakowitz, A. J. *Proc. Natl. Acad. Sci. U.S.A.* **2013**, *110*, 16315−16320.
(11) Bässler, H. *Phys. Status Solidi B* **1993**, *175*, 15.
(12) Pasveer, W.; Cottaar, J.; Tanase, C.; Coehoorn, R.; Bobbert, P.; Blom, P.; de Leeuw, D.; Michels, M. *Phys. Rev. Lett.* **2005***94*.
(13) Young, R. H. *Philos. Mag., Part B* **1995**, *72*, 435−457.
(14) Dunlap, D. H.; Parris, P. E.; Kenkre, V. M. *Phys. Rev. Lett.* **1996**, *77*, 542.
(15) Devizis, A.; Meerholz, K.; Hertel, D.; Gulbinas, V. *Phys. Rev. B* **2010**, *82*, 1555204.
(16) Kratky, O.; Porod, G. *Recl. Trav. Chim. Pay. B* **1949**, *68*, 1106−1122.
(17) Saito, N.; Takahashi, K.; Yunoki, Y. *J. Phys. Soc. Jpn.* **1967**, *22*, 219.
(18) Marcus, R. A. *J. Chem. Phys.* **1956**, *24*, 966−978.
(19) Troisi, A. *Org. Electron.* **2011**, *12*, 1988−1991.
(20) Grozema, F. C.; Siebbeles, L. D. A. *J. Phys. Chem. Lett.* **2011**, *2*, 2951−2958.
(21) Prins, P.; Grozema, F. C.; Schins, J. M.; Patil, S.; Scherf, U.; Siebbeles, L. D. A. *Phys. Rev. Lett.* **2006**, *96*, 146601.
(22) Pingel, P.; Zen, A.; Abellón, R. D.; Grozema, F. C.; Siebbeles, L. D.; Neher, D. *Adv. Funct. Mater.* **2010**, *20*, 2286−2295.
(23) Gasperini, A.; Sivula, K. *Macromolecules* **2013**, *46*, 9349−9358.
(24) Giri, G.; Verploegen, E.; Mannsfeld, S. C. B.; Atahan-Evrenk, S.; Kim, D. H.; Lee, S. Y.; Becerril, H. A.; Aspuru-Guzik, A.; Toney, M. F.; Bao, Z. *Nature* **2011**, *480*, 504−508.
(25) Zhu, R.; Kumar, A.; Yang, Y. *Adv. Mater.* **2011**, *23*, 4193−4198.
(26) Brinkmann, M.; Hartmann, L.; Biniek, L.; Tremel, K.; Kayunkid, N. *Macromol. Rapid Commun.* **2014**, *35*, 9−26.
(27) Kirkpatrick, S. *Phys. Rev. Lett.* **1971**, *27*, 1722.
(28) Kirkpatrick, S. *Rev. Mod. Phys.* **1973**, *45*, 574.
(29) Tessler, N.; Preezant, Y.; Rappaport, N.; Roichman, Y. *Adv. Mater.* **2009**, *21*, 2741−2761.
(30) Ambegaokar, V.; Halperin, B. I.; Langer, J. S. *J. Non-Cryst. Solids* **1972**, *8*, 492−496.
(31) Carbone, P.; Troisi, A. *J. Phys. Chem. Lett.* **2014**, *5*, 2637−2641.
(32) Hu, T.; Grosberg, A.; Shklovskii, B. *Phys. Rev. B* **2006***73*.

DOI: 10.1021/acsmacrolett.5b00314
ACS Macro Lett. 2015, 4, 708−712